

Thermal conduction in molecular chains: Non-Markovian effects

Dvira Segal

*Chemical Physics Theory Group, Department of Chemistry,
University of Toronto, 80 St. George Street, Toronto, Ontario M5S 3H6, Canada*
(Dated: October 29, 2018)

We study the effect of non-Markovian reservoirs on the heat conduction properties of short to intermediate size molecular chains. Using classical molecular dynamics simulations, we show that the distance dependence of the heat current is determined not only by the molecular properties, rather it is also critically influenced by the spectral properties of the heat baths, for both harmonic and anharmonic molecular chains. For highly correlated reservoirs the current of an anharmonic chain may exceed the flux of the corresponding harmonic system. Our numerical results are accompanied by a simple single-mode heat conduction model that can capture the intricate distance dependence obtained numerically.

PACS numbers:

I. INTRODUCTION

The problem of heat conduction through molecular structures has recently attracted lot of attention [1, 2, 3, 4, 5, 6] with potential applications in thermal machinery [7, 8], information processing and computation [9, 10], and thermoelectricity [11, 12].

One of the major open questions here is what are the factors that dominate thermal transport, the molecular structure, the contacts, or both [3]? Another central issue is the determination of the system size (N) dependence of the heat current J . While Fourier's law suggests the relation $J \propto N^{-1}$, extensive studies of heat flow in low dimensional systems have resolved a $J \propto N^{-\alpha}$ behavior, where α usually deviates from 1 [13]. Specifically, for harmonic chains one gets $\alpha = 0$ in the Markovian limit [14], i.e. the heat current does not depend on system size. This ballistic behavior results from the lack of scattering mechanisms between normal modes. In the harmonic limit the heat current thus reflects the spectral properties of the thermal reservoirs. In other words, it crucially depends on the details of the boundary conditions [15, 16]. In contrast, in strongly anharmonic systems where local thermal equilibrium exists, one expects that the steady state energy current will not depend on the properties of the contacts.

Recent studies of heat transport in disordered low-dimensional harmonic chains have manifested the influential role of the contacts' spectral properties on the asymptotic α value [15, 17]. Subsequent works exemplified this effect within anharmonic lattices [18, 19]. While these works have typically focused on the asymptotic length behavior, our objective here is to systematically study the effect of the reservoirs' spectral properties on the thermal transport in *short to intermediate* size molecular junctions that are of experimental relevance.

Using classical molecular dynamics simulations, we analyze the distance dependence of the current and the chain's temperature profile for Markovian and non-Markovian thermal baths considering either harmonic or anharmonic internal molecular interactions. We find that

the spectral properties of the reservoirs play a crucial role in determining the size dependence of the thermal current. Thus, one should carefully interpret experimental results [3], as both molecular structure and the properties of the boundaries critically determine the junction conductivity. Another interesting finding is that for highly correlated noise, anharmonic chains conduct more effectively than the corresponding harmonic systems. We qualitatively explain our numerical results using a single-mode heat conduction model that can be solved analytically [20, 21].

II. MOLECULAR DYNAMICS SIMULATIONS

We present here detailed classical molecular dynamics simulations of steady state heat transfer through one-dimensional (1D) molecular chains coupled to non-Markovian reservoirs. We model the molecule as a chain of N identical atoms. The end particles 1 and N are connected to heat baths of temperatures T_L and T_R respectively. The dynamics is governed by the generalized Langevin equation

$$\begin{aligned}\ddot{x}_k(t) &= -\frac{1}{m} \frac{\partial H_0}{\partial x_k}, \quad k = 2, 3, \dots, N-1 \\ \ddot{x}_1(t) &= -\frac{1}{m} \frac{\partial H_0}{\partial x_1} - \int_0^t dt' \gamma_L(t-t') \dot{x}_1(t') + \eta_L(t), \\ \ddot{x}_N(t) &= -\frac{1}{m} \frac{\partial H_0}{\partial x_N} - \int_0^t dt' \gamma_R(t-t') \dot{x}_N(t') + \eta_R(t).\end{aligned}\tag{1}$$

x_k is the position of the k particle of mass m , and p_k [see Eq. (5)] is the particle momentum. H_0 is the internal molecular Hamiltonian. γ_L and γ_R are friction constants and η_L and η_R are fluctuating forces that represent the effect of the thermal reservoirs. These terms are related through the fluctuation-dissipation relation ($n = L, R$)

$$\langle \eta_n \rangle = 0; \quad \langle \eta_n(t) \eta_n(t') \rangle = \frac{k_B T_n}{m} \gamma_n(t-t'), \tag{2}$$

where k_B is the Boltzmann constant. We consider here an exponentially correlated Ornstein-Uhlenbeck (O-U) noise [22]

$$\gamma_n(t-t') = \frac{\epsilon_n}{\tau_c^n} e^{-|t-t'|/\tau_c^n}, \quad (3)$$

with the intensity ϵ and a correlation time τ_c . For short correlation times the heat baths generate an uncorrelated (white) noise, $\gamma_n(t-t') \xrightarrow{\tau_c^n \rightarrow 0} 2\epsilon_n \delta(t-t')$. The Fourier transform of the O-U correlation function, to be used below, is

$$\gamma_n(\omega) \equiv \int e^{-i\omega t} \gamma_n(t) dt = \frac{2\epsilon_n}{1 + (\omega\tau_c^n)^2}. \quad (4)$$

A simple approach for implementing the O-U noise in numerical simulations is to introduce auxiliary dynamical variables $y_1(t)$ and $y_N(t)$ for the L and R baths respectively [23]. The new equations of motion for the first particle are

$$\begin{aligned} \dot{x}_1(t) &= \frac{p_1(t)}{m} \\ \ddot{x}_1(t) &= -\frac{1}{m} \frac{\partial H_0}{\partial x_1} - y_1(t) + \eta_L(t) \\ \dot{y}_1(t) &= -\frac{y_1(t)}{\tau_c^L} + \frac{\epsilon_L}{m\tau_c^L} p_1(t) \\ \dot{\eta}_L(t) &= -\frac{\eta_L(t)}{\tau_c^L} + \frac{1}{\tau_c^L} \sqrt{\frac{2\epsilon_L k_B T_L}{m}} \mu_L(t), \end{aligned} \quad (5)$$

where $\mu_L(t)$ is a Gaussian white noise, $\langle \mu_L(t) \rangle = 0$ and $\langle \mu_L(t) \mu_L(t') \rangle = \delta(t-t')$. An equivalent set of equations exists for the N particle, interacting with the R thermal bath. The coupled equations, Eq. (1) for particles $2..N-1$ and (5) with its N equivalent, are integrated using the fourth order Runge-Kutta method to yield the positions and velocities of all particles. The heat flux can be calculated from the trajectory using [13]

$$J = \frac{1}{2(N-1)} \sum_{k=1}^{N-1} \langle (v_k + v_{k+1}) F(x_{k+1} - x_k) \rangle, \quad (6)$$

where $F(r) = -dH_0(r)/dr$, $v_k = p_k/m$, and we average over time after steady state is achieved.

We describe next the molecular structure of the chain. We model the interactions between the atoms using a Morse potential of dissociation energy D , width α , and an interatomic equilibrium separation x_{eq} ,

$$H_0 = \sum_{k=1}^N \frac{p_k^2}{2m} + D \sum_{k=1}^N \left[e^{-\alpha(x_{k+1} - x_k - x_{eq})} - 1 \right]^2. \quad (7)$$

We consider two sets of parameters: In the first case the potential width is taken to be very small $\alpha \ll 1$, so as the potential energy is practically harmonic with a force constant $2D\alpha^2$. We refer to this model as "harmonic".

We also use parameters where the anharmonic coefficient is large, α/\sqrt{mD} of order 1. We refer to the later case as "anharmonic".

Unless otherwise stated, in the numerical simulation presented below we have typically used the following parameters: $D = 367.8/\nu^2$ kJ/mol, $\alpha = 1.875\nu$ Å⁻¹, $x_{eq} = 1.54$ Å, and $m=12$ gr/mole. These numbers describe a c-c stretching mode for $\nu = 1$ [24]. We take $\nu = 0.01$ for the harmonic model, while in the anharmonic case we use $\nu = 6$. We also assume that the two reservoirs have the same type of spectral function (O-U) with equal strength $\epsilon = \epsilon_n$ and noise correlation time $\tau_c = \tau_c^n$. Depending on the situation, we have used integration time step $\Delta t = 10^{-3} - 10^{-4}$ 1/ ω , where ω is the molecular frequency in the harmonic limit. We also take care of the required inequality $\Delta t \ll \tau_c$.

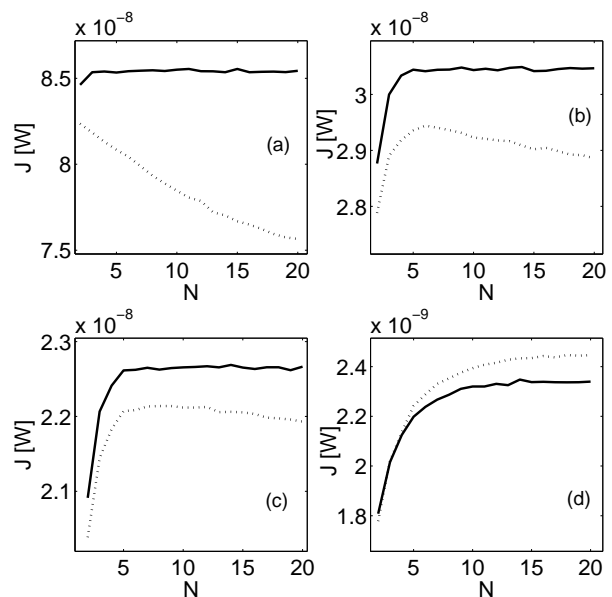


FIG. 1: Distance dependence of the heat current in non-Markovian systems for harmonic (full), and anharmonic (dotted) models. (a) Gaussian white noise; (b) O-U noise with $\tau_c=8 \times 10^{-3}$ ps; (c) O-U noise with $\tau_c = 0.01$ ps; (d) O-U noise with $\tau_c=0.04$ ps. $T_R = 300K$, $T_L = 0K$, $\epsilon = 50$ ps⁻¹ in all cases.

Figure 1 presents the heat current for harmonic (J_H) and anharmonic (J_A) chains calculated with different memory times τ_c . Panel (a) shows the heat current in the Markovian limit. We find that the energy flux in harmonic systems does not depend on size, while it decays with distance for anharmonic chains in agreement with standard results [13]. When the noise correlation time is increased, an interesting behavior is observed [panel (b)]: While J_H remains a constant to a good approximation, the anharmonic flux manifests an initial rise, followed by a decay for long enough chains. As the memory time is further increased (c), the current of an anharmonic system saturates, and is approximately a constant over the relevant sizes. This observation interestingly shows a

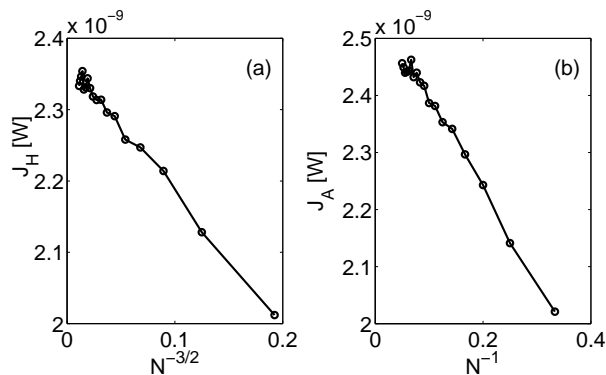


FIG. 2: Resolving the distance dependence of the thermal current in non-Markovian O-U systems for harmonic (a) and anharmonic (b) models, $\tau_c=0.04$ ps, $T_R = 300K$, $T_L = 0K$, $\epsilon = 50$ ps $^{-1}$.

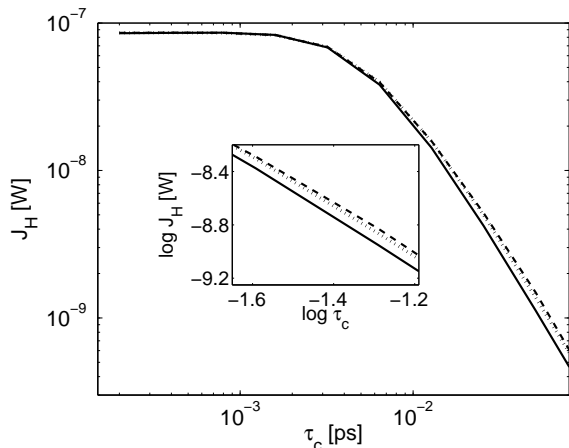


FIG. 3: Decrease of heat current with increasing bath correlation time for harmonic systems. $T_R = 300K$, $T_L = 0K$, $\epsilon = 50$ ps $^{-1}$. $N=2$ (full), $N = 5$ (dotted), $N = 10$ (dashed). The inset zooms on the high τ_c values.

counteracting effect between the molecular contribution to the heat current and the reservoirs spectral properties. For highly correlated reservoirs (d) both harmonic and anharmonic currents are slightly enhanced with distance. Surprisingly, in this case the anharmonic junction conducts better than a fully harmonic system.

We explain next these observations. First we clarify why J_H - and J_A for short chains- increase with N for non-Markovian baths. As was shown in Ref. [25] the dominant heat conducting vibrational modes of alkane chains are shifted towards lower frequencies with increasing molecular size. Since within the O-U model $\gamma(\omega)$ (reflecting the system-bath coupling) is larger at lower frequencies, the current gets enhanced with distance.

Next we explain the intricate current-distance behavior of anharmonic systems. Anharmonic interactions lead to scattering processes between the molecular modes. These scattering effects are more influential with increas-

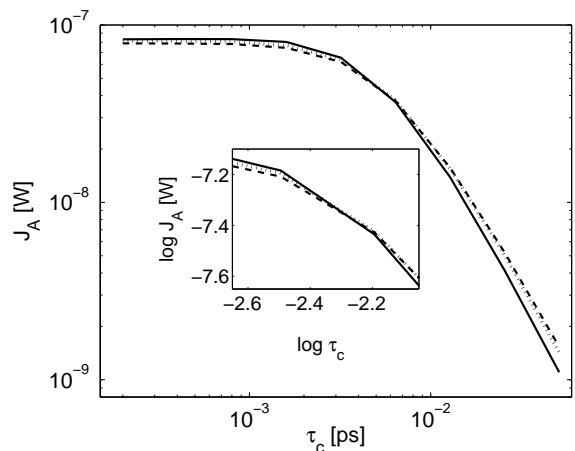


FIG. 4: Decrease of heat current with increasing bath correlation time for an anharmonic molecular model. $N=2$ (full), $N = 5$ (dotted), $N = 10$ (dashed). $T_R = 300K$, $T_L = 0K$, $\epsilon_n = 50$ ps $^{-1}$. The inset zooms on intermediate τ_c values where J_A is independent of length.

ing chain length. In Markovian systems this results in the enhancement of the junction resistance, thus it leads to the reduction of current with N . However, in non-Markovian systems these scattering effects are actually beneficial for transferring energy from molecular modes which are above the reservoirs' cutoff frequencies, into low energy modes that overlap with the solids vibrations. The interplay between these two effects leads to a rich behavior: If τ_c^{-1} is higher than the molecular frequencies, here of the order of 150 ps $^{-1}$, anharmonic effects lead to the reduction of current with size, see panels (a)-(b). In the opposite small cutoff limit (d), $\tau_c^{-1} = 25$ 1/ps, harmonic systems can transfer only those modes that are in the reservoirs energy window, while anharmonic junctions better conduct by scattering high energy modes into low frequencies. For $\tau_c \sim 0.01$ ps the two effects practically cancel and J_A weakly depends on distance (c).

Fig. 2 presents the distance dependence of the energy flux for both harmonic and anharmonic chains assuming solids of long memory time, $\tau_c = 0.04$ ps. While it is difficult to make a definite conclusion, we find that J_H and J_A obey different functional forms.

Next we systematically explore the dependence of the heat flux on the reservoirs' correlation time. Figs. 3 and 4 manifest that the Markovian behavior sustains for times up to $\tau_c \sim 5 \times 10^{-3}$ ps. For longer correlation times the heat current significantly decays with τ_c for both harmonic and anharmonic chains. The inset of Fig. 4 further shows that for $\tau_c \sim 6 \times 10^{-3}$ ps the anharmonic heat flux is practically distance independent, see also Fig. 1(c). As discussed above, this intriguing behavior results from an effective cancellation between internal molecular interactions, leading to the decay of current with N , and the reservoirs properties, which can lead to an enhancement of current with distance. In the next section we present a simple analytical model that can capture this

intricate behavior.

In Fig. 5 we study the temperature dependence of the heat current for both Markovian and non-Markovian chains for a representative length $N=8$. We find that both harmonic and anharmonic systems show a linear current-temperature relationship in the range $T = 0-300$ K. The thermal conductance ($J/\Delta T$) calculated from Figs. 1-4 is therefore approximately independent of temperature.

We have also analyzed in Fig. 6 the ϵ dependence of the current for Markovian and O-U systems, and found an approximate linear relation in the low dissipation regime. For Markovian baths the current decreases as ϵ^{-1} when the coupling is strong, $\epsilon > 100$ ps $^{-1}$. We expect that the colored noise model will demonstrate a similar behavior for very strong molecule-bath interactions [19].

We conclude this section by noting that the qualitative behavior observed above (Figs. 1-4) applies for a broad range of temperatures and coupling parameters. We expect that similar characteristics will be discovered in molecular systems of various anharmonic internal interactions.

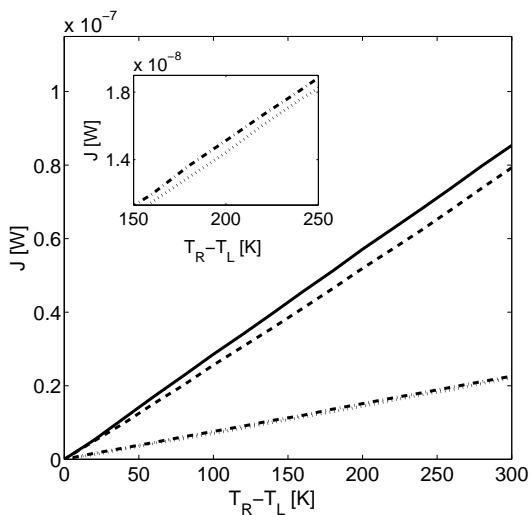


FIG. 5: Temperature dependence of the thermal flux, $N=8$, $T_R=300$ K. Harmonic chain with white noise (full); Anharmonic chain with white noise (dashed); Harmonic chain with O-U noise, $\tau_c=0.01$ ps, $\epsilon=50$ ps $^{-1}$ (dashed-dotted); Anharmonic chain with O-U noise, $\tau_c=0.01$ ps, $\epsilon=50$ ps $^{-1}$ (dotted). The inset zooms on the O-U simulations.

III. SINGLE-MODE HEAT CONDUCTION MODEL

We present here a simple model that yields a qualitative explanation for the influential role of non-Markovian reservoirs on the heat transfer properties of short to intermediate ($N = 2 - 20$) molecular chains. In our simple picture, heat current in a linear molecular system is dominated by a specific vibrational mode of fre-

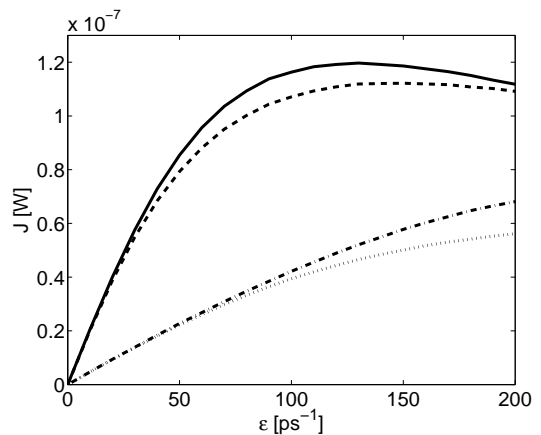


FIG. 6: Thermal flux as a function of system-bath coupling strength ϵ , $T_R=300$ K, $T_L=0$ K. Parameters and lines setting are the same as in Fig. 5.

quency ω_0 . The total Hamiltonian includes three terms, $H = H_B + H_0 + H_I$, where for a harmonic local mode

$$\begin{aligned} H_B &= \sum_{j,n} \frac{p_{j,n}^2}{2m_j} + \frac{1}{2} m_j \omega_j^2 q_{j,n}^2 \\ H_0 &= \frac{p_0^2}{2M} + \frac{M\omega_0^2 q_0^2}{2} \\ H_I &= \sum_{j,n} \lambda_{j,n} q_{j,n} q_0. \end{aligned} \quad (8)$$

H_B includes two thermal reservoirs $n = L, R$ of different temperatures, each consisting a set of independent harmonic oscillators with masses m_j , coordinates $q_{j,n}$, and momenta $p_{j,n}$. H_0 represents the (single) relevant molecular mode with coordinate q_0 , momentum p_0 , mass M and frequency ω_0 . It can be written equivalently in the energy representation as $H_0 = \sum_{l=0,1,2,\dots} l\omega_0 |l\rangle\langle l|$; $\hbar \equiv 1$. If we sum over states up to infinity ($l\omega_0 \gg T_n$), this term describes a harmonic mode as in Eq. (8). We can also model an anharmonic molecule by truncating the single mode spectrum to include only few vibrational states [20, 21]. The system-bath interaction is taken to be bilinear, with $\lambda_{j,n}$ as the coupling constant.

Assuming weak molecule-bath coupling at both ends, an analytical expression for the heat current in steady state can be derived using the master equation formalism [20, 21]. In the harmonic limit and at high temperatures ($T > \omega_0$) the thermal current is given by a Landauer type expression [20]

$$J_H = \frac{\gamma_L(\omega_0)\gamma_R(\omega_0)}{\gamma_L(\omega_0) + \gamma_R(\omega_0)} k_B \Delta T, \quad (9)$$

where $\Delta T = T_R - T_L$ and $\gamma_n(\omega) = \frac{\pi}{2} \sum_j \frac{\lambda_{j,n}^2}{M m_j \omega_j^2} \delta(\omega - \omega_j)$ is the Fourier transform of the friction constant $\gamma_n(t)$ (1) [26]. The memory damping can be also expressed in terms of the reservoir's spectral function $g_n(\omega) =$

$2\pi \sum_j \frac{\lambda_{j,n}^2}{M m_j \omega_j} \delta(\omega - \omega_j)$ as $\gamma_n(\omega) = g_n(\omega)/4\omega$. Equation (9) clearly manifests that in the harmonic limit the heat current is exclusively determined by the spectral properties of the reservoirs. This behavior results from the lack of scattering mechanisms in the harmonic system.

As mentioned above, within this simple picture we can also model a highly anharmonic molecule by truncating the single mode spectrum. For a two-level model ($l=0,1$) at high temperatures the heat current is given by [20]

$$J_A = \frac{\gamma_L(\omega_0)\gamma_R(\omega_0)}{\gamma_L(\omega_0) + \gamma_R(\omega_0)} \frac{\omega_0}{2T_B} \Delta T, \quad (10)$$

where the temperature of the local model (sometimes referred to as a bridge B) is

$$T_B = \frac{\gamma_L(\omega_0)T_L + \gamma_R(\omega_0)T_R}{\gamma_L(\omega_0) + \gamma_R(\omega_0)}. \quad (11)$$

Though expressions (9) and (10) provide the heat current for a simplistic model, they may serve us for gaining qualitative understanding of heat transfer in an N -sites molecule. The key element here is the observation that in short linear chains relatively few modes contribute to the transport of thermal energy [25]. For simplicity, we may assume that a *single mode* dominates the dynamics, and use the following generic form to describe its size dependence

$$\omega_0 \approx \omega_M \left(1 + \frac{\beta}{N}\right). \quad (12)$$

ω_M is the asymptotic frequency for large N , β is a constant that is specific for the material. Note that Eq. (12) does not necessarily describe the variation of the lowest vibrational mode of the chain with increasing length. Rather, this is a qualitative expression for the variation of the *dominant* heat conducting mode with size: For short chains the spectrum is significantly altered with size. For large enough chains ω_0 is approximately fixed.

We can clearly discern in Eqs. (9)-(10) the role of different factors (contacts and internal interactions) in determining the heat current. While the reservoirs spectral properties enter these expressions through the damping rate γ , calculated at the relevant molecular frequency ω_0 , anharmonic interactions yield an extra ω_0/T_B factor that accounts for the local mode occupancy. Since both of these terms depend on frequency, thus on size through Eq. (12), the resulting N dependence is not trivial. We study next various models for the damping element, Markovian and non-Markovian, assuming for simplicity that the system is symmetric with respect to the two ends, $\gamma = \gamma_n$ ($n = L, R$).

I. Markovian process. For a Markovian process the spectral function is Ohmic, $g(\omega) = 4\epsilon\omega$, thus the friction is a constant, $\gamma(\omega) = \epsilon$. In this limit Eqs. (9) and (10) reduce to

$$\begin{aligned} J_H^{(M)} &= \frac{\epsilon}{2} k_B \Delta T \\ J_A^{(M)} &= \frac{\epsilon \Delta T \omega_M}{2(T_L + T_R)} \left(1 + \frac{\beta}{N}\right). \end{aligned} \quad (13)$$

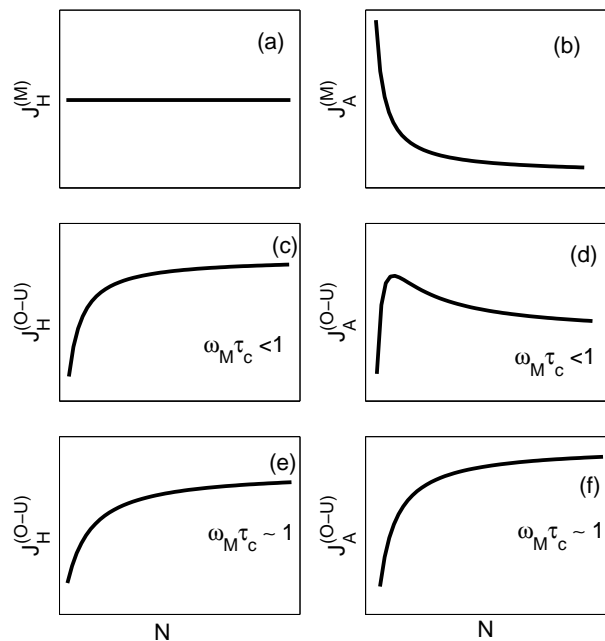


FIG. 7: Qualitative behavior of the heat current in the single-mode heat conduction model for Markovian and non-Markovian reservoirs. (a)-(b) Heat current for a Gaussian white noise [Eq. (13)]; (c)-(d) Current for an O-U noise with a short memory time, Eq. (14) with $\omega_M \tau_c < 1$; (e)-(f) Current for an O-U noise with a long memory time, Eq. (14) with $\omega_M \tau_c \sim 1$.

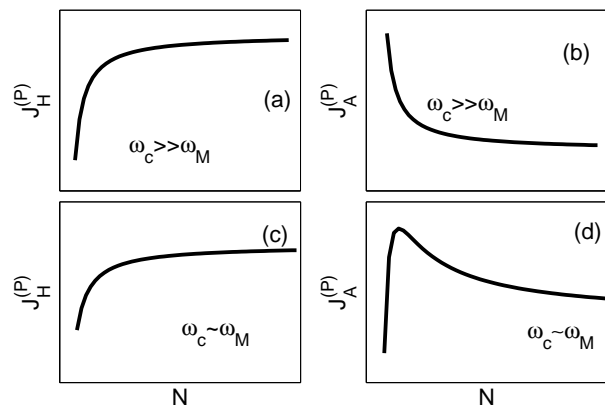


FIG. 8: Qualitative behavior of heat current in the single-mode heat conduction model with a power law spectral function (15), $s = 1$.

These expressions are consistent with standard results [13]: The current in harmonic systems does not depend on size, while in anharmonic models it decays with distance. In Fig. 7 (a)-(b) we qualitatively exemplify this behavior by simulating Eq. (13), reproducing the results of panels (a)-(b) of Fig. 1.

II. Ornstein-Uhlenbeck noise. The exponentially correlated (O-U) process $\gamma(t) = \epsilon/\tau_c e^{-|t|/\tau_c}$ transforms into a Lorentzian in frequency domain, $\gamma(\omega) = \frac{2\epsilon}{1+\omega^2\tau_c^2}$. The

fluxes (9) and (10) then become ($\epsilon = \epsilon_n$ and $\tau_c = \tau_c^n$)

$$\begin{aligned} J_H^{(O-U)} &= \frac{k_B \Delta T \epsilon}{1 + \omega_0^2 \tau_c^2} \propto \left(1 - \frac{\beta}{N}\right)^2 \\ J_A^{(O-U)} &= \frac{\Delta T}{T_L + T_R} \frac{\epsilon \omega_0}{1 + \omega_0^2 \tau_c^2} \propto \left(1 - \frac{\beta}{N}\right), \end{aligned} \quad (14)$$

where we derived the approximate distance dependence by assuming that $\omega_0 \tau_c > 1$ and taking $\beta/N < 1$. These expressions clearly demonstrate an *enhancement* of the current with N for both harmonic and anharmonic systems when the reservoirs have (each) a highly correlated noise.

In Fig. 7 (c)-(f) we simulate Eq. (14). For short correlation time we reproduce the results of Fig. 1(b), manifesting an enhancement of the anharmonic flux followed by a decrease of current. For very long correlation times the current systematically increases with size, in agreement with the numerical data, Fig. 1 (d).

III. Power law models. The spectral function $g(\omega) = \epsilon \omega^s e^{-\omega/\omega_c}$ is a widely accepted description of solids, ω_c is the reservoir cutoff frequency. Unlike the O-U noise which satisfies the differential equations (5), this noise cannot be reduced into a multi-component Markovian process, thus it is not trivial to simulate [27]. Within the single-mode heat conduction model the heat current for harmonic and anharmonic modes (9)-(10) is given by

$$\begin{aligned} J_H^{(P)} &= \frac{\epsilon}{2} k_B \Delta T \omega_0^{s-1} e^{-\omega_0/\omega_c} \\ J_A^{(P)} &= \epsilon \frac{\Delta T}{2(T_L + T_R)} \omega_0^s e^{-\omega_0/\omega_c}, \end{aligned} \quad (15)$$

where ω_0 is the dominant frequency for heat transport (12). For an Ohmic ($s = 1$) bath, taking $\omega_c \gg \omega_0$, the dynamics reduces to the Markovian limit (13), where $J_H^{(P)}$ is weakly enhanced with distance and $J_A^{(P)}$ decays with N . This behavior is exemplified in Fig. 8 (a)-(b). In contrast, for $\omega_c \sim \omega_0$, a different trend is observed: while $J_H^{(P)}$ monotonically increases with length (c), in anharmonic systems the current first increases with size, then falls down (d). For $s = 2$ we expect that, quite interestingly, the heat current in harmonic models will *decay* with distance. This is because for long chains the dominant conducting frequencies are red shifted, while the solid spectral function is maximal at ω_c .

We conclude that short to intermediate size molecular chains coupled to general environments can manifest a rich behavior: The thermal current can either increase or decrease with size, critically depending both on the molecular internal interactions and on the reservoirs spectral properties. Despite its simplicity, the model presented here provides a useful starting point for explaining the complicated behavior observed within atomistic classical molecular dynamics simulations. In the next section we show that this model is also a useful tool for estimating the temperature profile along molecule.

IV. TEMPERATURE PROFILE

We investigate next the effect of the reservoirs spectral properties on the local temperature profile in harmonic and anharmonic chains. Within the single mode heat conduction model one can define in steady state the temperature of the local mode as $k_B T_B = \omega_0 \sum_l l P_l$, where P_l is the population of the l vibrational state. In the classical limit it can be shown that this expression reduces to Eq. (11), $T_B = \frac{\gamma_L(\omega_0)T_L + \gamma_R(\omega_0)T_R}{\gamma_L(\omega_0) + \gamma_R(\omega_0)}$, for both harmonic and anharmonic local modes [20, 21]. We therefore expect that when the reservoirs have the same type of spectral function with the same coefficients, the temperature profile is independent of the type, and is given by the arithmetic average $T_B = (T_L + T_R)/2$. On the other hand, when the two reservoirs have different types of spectral densities (or different memory times), the temperature profile along the chain depends on the model. For example, if $T_L \ll T_R$ and $\gamma_R \ll \gamma_L$, $T_B \sim \gamma_R T_R / \gamma_L \ll T_R$. In contrast, for $T_L \ll T_R$ but $\gamma_R > \gamma_L$, $T_B \sim T_R$. This behavior was observed by Saito et al. in the harmonic limit using a quantum master equation formalism [16].

Using classical molecular dynamics simulations we compute the temperature profile by calculating the mean kinetic energy for each particle, $T_k = \langle \frac{p_k^2}{2m} \rangle \frac{2}{k_B}$. Here p_k is the momentum of the k th particle calculated after steady state develops, and we average over time and initial configurations using the procedure and parameters of section II.

Fig. 9 manifests that the bulk temperature profile is close to the arithmetic average (150 K) for both Markovian and non-Markovian systems when the reservoirs are identical. At the boundaries we see interesting features noted earlier in Refs. [14, 16, 28, 29]: The temperature close to the cold end (L) slightly rises, even to values higher than the average temperature. For an anharmonic system a small temperature gradient develops at the chain center. This effect is more pronounced for Markovian reservoirs. Note that in Markovian harmonic systems the temperature at the chain center, e.g. T_{10} , is higher than the anharmonic value. This trend is reversed for O-U baths, as here anharmonic interactions facilitate equilibration with the slow environment.

We employ next reservoirs of different spectral properties, and study the heat current and temperature profile in this asymmetric system. We assume that both reservoirs are of O-U type, but take different memory times $\tau_c^L \neq \tau_c^R$. Fig. 10 manifests that the current in a harmonic system is independent of the direction of the asymmetry, i.e. if the cold bath is weakly or strongly coupled to the molecule. In contrast, the current in an anharmonic chain is significantly altered when the asymmetry is reversed: It is higher when the hot bath is slow. This response to spatial asymmetry is the underlying principle of the "thermal rectifier" [4, 20, 30].

Fig. 11 shows that the bridge temperature dramatically responds to the direction of the asymmetry for *both*

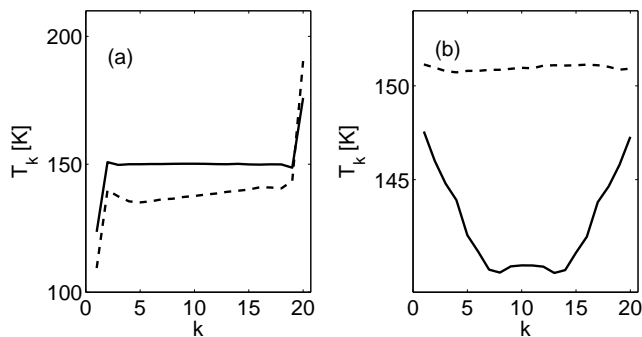


FIG. 9: Temperature profile along harmonic (full) and anharmonic (dashed) chains coupled to reservoirs of identical spectral properties. (a) Gaussian white noise; (b) O-U noise with $\tau_c = 0.04$ ps. $N=20$, $T_R=300$ K, $T_L=0$ K and $\epsilon = 50$ ps $^{-1}$ in all cases.

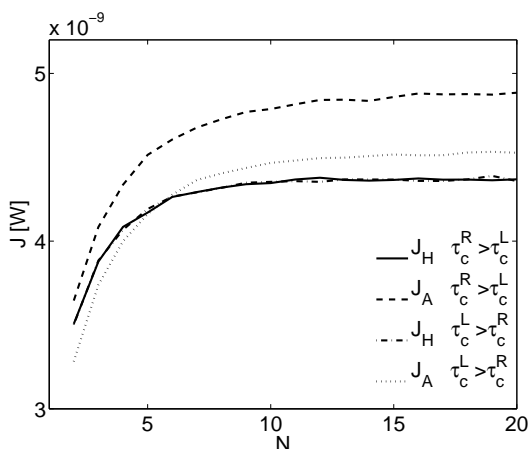


FIG. 10: Heat current in molecular chains coupled to reservoirs of different spectral properties $\tau_c^L \neq \tau_c^R$, $\epsilon_L = \epsilon_R = 50$ ps $^{-1}$. $\tau_c^L = 0.002$ ps, $\tau_c^R = 0.04$ ps: harmonic (full); anharmonic (dashed). $\tau_c^L = 0.04$ ps, $\tau_c^R = 0.002$ ps: harmonic (dashed-dotted); anharmonic (dotted). $T_R=300$ K and $T_L=0$ K in all cases.

harmonic and anharmonic systems. We find that it is close to the temperature of the reservoir with the short memory time. In other words, the molecule better equilibrates with the Markovian reservoir. This behavior is consistent with the results of Ref. [16], and qualitatively agrees with Eq. (11).

V. DISCUSSION AND SUMMARY

In this paper we have investigated the effect of the contacts' spectral properties on the thermal conduction of harmonic and anharmonic short to intermediate size chains using classical molecular dynamics simulations.

When the system size is smaller than the mean free path, heat conduction is dominated by harmonic interactions. In such systems the spectral properties of the

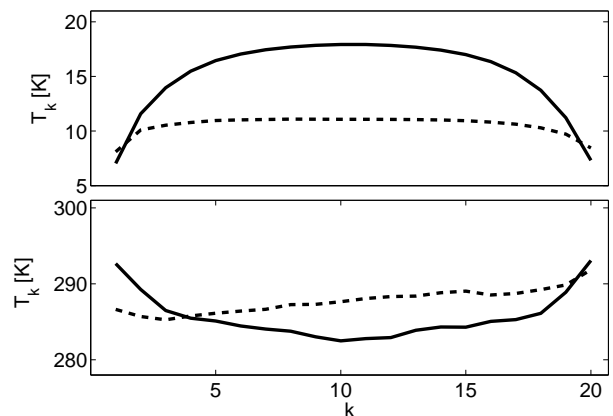


FIG. 11: Temperature profile along harmonic (full) and anharmonic (dashed) chains coupled to reservoirs of different spectral properties $\tau_c^L \neq \tau_c^R$, $\epsilon_L = \epsilon_R = 50$ ps $^{-1}$. $\tau_c^R = 0.04$ ps, $\tau_c^L = 0.002$ ps (top); $\tau_c^R = 0.002$ ps, $\tau_c^L = 0.04$ ps (bottom). The temperature profile was calculated for an $N = 20$ sites chain using $T_R=300$ K, $T_L=0$ K in all cases.

contacts play a central role in determining the dynamics in the junction. We found that the distance dependence of the current strongly varies with the baths (noise) correlation time: While for Markovian baths the current in harmonic systems is independent of size, it slightly increases with length when the reservoirs have long memory. The effect is even more dramatic in anharmonic chains. Here the current decays with N in the Markovian limit, while it gets enhanced with distance when the reservoirs have long memory times.

Other interesting observations are: (i) We identified a regime where the anharmonic flux is practically distance independent due to the counteracting effects of molecular nonlinearities and bath correlations. (ii) For long memory times the current through anharmonic chains might be higher than the analogous harmonic current. Thus, anharmonic interactions might play a surprising role, enhancing the heat flux across molecules coupled to non-Markovian reservoirs. We also showed that the single-mode heat conduction model developed in Ref. [20] can essentially capture the length dependence and the temperature profile obtained within classical molecular dynamics simulations.

Before we conclude we briefly discuss the relationship of our calculations to relevant experiments. Wang et al. have recently measured the thermal conductance ($\mathcal{K} = J/A\Delta T$, \mathcal{A} is the cross section) of 8-10 alkandithiols monolayers [3]. The values $\mathcal{K} \sim 25-28$ MWm $^{-2}$ K $^{-1}$ were obtained, roughly independent of system size. Previous calculations [25] confirm this observation: The heat current of alkane chains is expected to be distance independent, even for very long ($N=100$) molecules, due to weak anharmonic internal interactions in the system. More quantitatively, Eq. (9) predicts thermal conductance of $\mathcal{K} \sim 280$ MWm $^{-2}$ K $^{-1}$, using Markovian thermal baths

with $\epsilon=10 \text{ ps}^{-1}$ and a cross section $\mathcal{A} = (5 \times 10^{-10})^2 \text{ m}^{-2}$. As discussed above, memory effects can reduce this number by 1-2 orders of magnitude. Therefore the conductance calculated here is in a reasonable agreement with experimental results.

Several future directions are of interest. First, we have restricted our discussion to the O-U correlation function, since it can be easily simulated as a multi-component Markovian process [23]. It is worth extending this study to include more realistic environments of ω^s spectral properties. This type of noise correlations can be simulated using the inverse Fourier transform technique [27, 31, 32]. Other interesting questions are what is the role of the contacts in higher dimensions, and how

do quantum mechanical effects alter the phenomena addressed in this paper [16, 25, 28, 29, 33, 34, 35].

Understanding thermal transport in molecule-solid interfaces is important for molecular electronic applications [36]. It is also an imperative step in the endeavor for developing unique molecular level thermal devices [8, 9, 10].

Acknowledgments

This work was supported by a University of Toronto Start-up Grant.

-
- [1] P. Kim, L. Shi, A. Majumdar, P. L. McEuen, *Phys. Rev. Lett.* **87**, 215502 (2001).
 - [2] Z. Ge, D. G. Cahill, P. V. Braun, *Phys. Rev. Lett.* **96**, 186101 (2006).
 - [3] R. Y. Wang, R. A. Segalman, A. Majumdar, *App. Phys. Lett.* **89**, 173113 (2006).
 - [4] C. W. Chang, D. Okawa, A. Majumdar, A. Zettl, *Science* **314**, 1121 (2006).
 - [5] Z. Wang, J. A. Carter, A. Lagutchev, Y. K. Koh, N.-H. Seong, D. G. Cahill, D. D. Dlott, *Science*, **317**, 787 (2007).
 - [6] C. Chiritescu, D. G. Cahill, N. Nguyen, D. Johnson, A. Bodapati, P. Keblinski, P. Zschack, *Science* **315**, 351 (2007).
 - [7] C. W. Chang, D. Okawa, H. Garcia, T. D. Yuzvinsky, A. Majumdar, A. Zettl, *App. Phys. Lett.* **90**, 193114 (2007).
 - [8] D. Segal, A. Nitzan, *Phys. Rev. E* **73**, 026109 (2006).
 - [9] L. Wang, B. Li, *Phys. Rev. Lett.* **99**, 177208 (2007).
 - [10] Z. Liu, B. Li, *Phys. Rev. E* **76**, 051118 (2007).
 - [11] P. Reddy, S.-Y. Jang, R. A. Segalman, A. Majumdar, *Science* **315**, 1568 (2007).
 - [12] A. I. Hochbaum, R. K. Chen, R. D. Delgado, W. J. Liang, E. C. Garnett, M. Najarian, A. Majumdar, P. D. Yang, *Nature* **451**, 163 (2008).
 - [13] S. Lepri, R. Livi, A. Politi, *Phys. Rep.* **377**, 1 (2003).
 - [14] Z. Rieder, J. L. Lebowitz, E. Lieb, *J. Math. Phys.* **8**, 1073 (1967).
 - [15] A. Dhar, *Phys. Rev. Lett.* **86**, 5882 (2001).
 - [16] K. Saito, S. Takesue, S. Miyashita, *Phys. Rev. E* **61**, 2397 (2000).
 - [17] L. Wee Lee, A. Dhar, *Phys. Rev. Lett.* **95**, 094302 (2005).
 - [18] H. Zhao, L. Yi, F. Liu, B. Xu, *Eur. Phys. J. B* **54**, 185 (2006).
 - [19] D. Barik, *Eur. Phys. J. B* **56**, 229 (2007).
 - [20] D. Segal, A. Nitzan, *Phys. Rev. Lett.* **94**, 034301 (2005); *J. Chem. Phys.* **122**, 194704 (2005).
 - [21] D. Segal, *Phys. Rev. B* **73**, 205415 (2006).
 - [22] G. E. Uhlenbeck, L. S. Ornstein, *Phys. Rev.* **36**, 823 (1930).
 - [23] J. Luczka, *Chaos* **15**, 026107 (2005).
 - [24] S. Lifson, P. S. Stern, *J. Chem. Phys.* **77**, 4542 (1982).
 - [25] D. Segal, A. Nitzan, P. Hänggi, *J. Chem. Phys.* **119**, 6840 (2003).
 - [26] P. Hänggi, *Lect. Notes Phys.* **484**, 15 (1997).
 - [27] R. F. Fox, I. R. Gatland, R. Roy, G. Vemuri, *Phys. Rev. A* **38**, 5938 (1988).
 - [28] U. Zürcher, P. Talkner, *Phys. Rev. A* **42**, 3278 (1990).
 - [29] A. Dhar, B. S. Shastry, *Phys. Rev. B* **67**, 195405 (2003).
 - [30] M. Terraneo, M. Peyrard, G. Casati, *Phys. Rev. Lett.* **88**, 094302 (2002).
 - [31] J.-D. Bao, Y.-Z. Zhuo, *Phys. Rev. E* **71**, 010102(R) (2005).
 - [32] X.-P. Zhang, J.-D. Bao, *Phys. Rev. E* **73**, 061103 (2006).
 - [33] A. Ozpineci, S. Ciraci, *Phys. Rev. B* **63**, 125415 (2001).
 - [34] N. Mingo, *Phys. Rev. B* **74**, 125402 (2006).
 - [35] J.-S. Wang, *Phys. Rev. Lett.* **99**, 160601 (2007).
 - [36] M. Galperin, A. Nitzan, M. A. Ratner, *Phys. Rev. B* **75**, 155312 (2007).